# Synthesis, Structure and Characterization of the New Complex $[L_1(H_2O)Fe(\mu\text{-}O)Fe(OH_2)L_1]^{4+}$ [$L_1$ = *N,N'*-Bis(1-methylimidazolyl-2-methyl)-*N,N'*-Bismethyl-1,2-ethanediamine] − Formation of the $(\mu\text{-}O)(\mu\text{-}H_3O_2)$ Complex upon Deprotonation

**Sandrine Poussereau,[a] Geneviève Blondin,*[a] Geneviève Chottard,[b] Jean Guilhem,[c] Luba Tchertanov,[c] Eric Rivière,[a] and Jean-Jacques Girerd[a]**

**Keywords:** Iron / Oxo complexes / Methane monooxygenase / UV/Vis spectroscopy / Raman spectroscopy

The compound $[L_1(H_2O)Fe(\mu\text{-}O)Fe(OH_2)L_1](ClO_4)_4\cdot 2H_2O$ [$\mathbf{1}(ClO_4)_4\cdot 2H_2O$] [$L_1$ = *N,N'*-bis(1-methylimidazolyl-2-methyl)-*N,N'*-bismethyl-1,2-ethanediamine] was synthesized. It is characterized by a linear Fe–(μ-O)–Fe motif with an Fe···Fe distance of 3.584(1) Å. The measurement of the magnetic susceptibility as a function of temperature indicated a strong antiferromagnetic coupling between the two high-spin $Fe^{III}$ ions ($J = -223$ $cm^{-1}$ with $H = -J\cdot S_1\cdot S_2$). In the solid state, the symmetric stretching vibration mode of the Fe–(μ-O)–Fe core unit was detected at 347 $cm^{-1}$, in agreement with a straight Fe–(μ-O)–Fe angle. Upon addition of up to one equivalent of triethylamine to an acetonitrile solution of **1**, conversion to the $[L_1(H_2O)Fe(\mu\text{-}O)Fe(OH)L_1]^{3+}$ complex **2** was observed. This last species was isolated as a perchlorate salt [$\mathbf{2}(ClO_4)_3\cdot H_2O$]. Susceptibility measurements and Raman and UV/Vis investigations on the powder and/or an acetonitrile solution confirmed the presence of an intramolecular hydrogen bond between the coordinated water molecule and the hydroxide group leading to a bent $[Fe(\mu\text{-}O)Fe]^{4+}$ core structure.

## Introduction

The oxidation of methane to methanol with dioxygen catalyzed by soluble methane monooxygenase (MMO) has elicited much interest during recent years. This reaction takes place in the hydroxylase component of MMO (MMOH),[1,2] the structure of which has been determined by X-ray diffraction studies in the native ($MMOH_{ox}$) and reduced ($MMOH_{red}$) forms for *Methylococcus capsulatus*,[3,4] and in the native form only for *Methylosinus tricosporium*.[5] The catalytic site determined in the two forms is constituted by two iron atoms bridged by the carboxylato group of a glutamate residue (E144). Both iron sites are in the +III oxidation state in $MMOH_{ox}$ and connected by two extra bridges: one water molecule and one hydroxide group.[4,5] In the reduced state, both metallic centers have the +II oxidation degree, a single oxygen atom of the carboxylate side function of the glutamate residue E243 being present as a second bridge.[4] The only exogeneous ligand is a water molecule that is coordinated to one $Fe^{II}$ site and that recent investigations in the catalytic cycle of the enzyme have brought to the fore. It has been suggested that one of its protons is transferred to one oxygen atom of the O−O bridge in the peroxo form of MMOH (compound P)[6,7] formed by reaction of $MMOH_{red}$ with dioxygen.[8−11] This would leave a hydroxo group ligated to one $Fe^{III}$ site or bridging the two metallic centers.[6,7] Compound P spontaneously converts to compound Q, which has been shown by Mössbauer and X-ray absorption studies to present a di-$Fe^{III}$-di-μ-oxo core unit.[12] It has been proposed that upon this evolution, a second proton is transferred from the hydroxide molecule to the hydrogenated peroxo bridge, allowing the release of a water molecule.[6,7] The two bridging oxygen atoms of the $[Fe_2(\mu\text{-}O)_2]^{4+}$ unit would thus have different origins, one coming from the dioxygen molecule and the other one being the doubly deprotonated coordinated water molecule present in $MMOH_{red}$. Compound Q is the active catalytic species that interacts with the alkane substrate.[6,8,9,13]

Many efforts have been made to synthesize dinuclear iron complexes presenting the diamond core structure. For this purpose, tetradentate ligands are used.[14−18] Starting with a $[(H_2O)Fe(\mu\text{-}O)Fe(OH)]^{3+}$ core unit, we have shown recently the possibility to obtain the double-bridged structure $[Fe(\mu\text{-}O)(\mu\text{-}OH)Fe]^{3+}$.[14] The protonated form of the diamond core structure is thus formed in the same way as would be the di-iron-di-μ-oxo unit of compound Q, an oxygenated group converting from a $\eta^1$- to a μ-type coordination. This behavior seems to be common to several systems.[14,16,19] In our effort to model the active site of MMOH, the synthesis of two new iron-oxo complexes with

---

[a] Laboratoire de Chimie Inorganique, UMR CNRS 8613,
Institut de Chimie Moléculaire d'Orsay, Université Paris-Sud,
91405 Orsay Cedex, France
Fax: (internat.) +33-1/6915-4754
E-mail: gblondin@icmo.u-psud.fr

[b] Laboratoire de Chimie Inorganique et Matériaux Moléculaires,
ESA CNRS 7071, Université Pierre et Marie Curie,
75250 Paris Cedex 05, France

[c] Institut de Chimie des Substances Naturelles, UPR CNRS 2301,
91198 Gif-sur-Yvette, France

1434−1948/01/0404−1057 $ 17.50+.50/0

the tetradentate ligand containing imidazole groups *N,N'*-bis(1-methylimidazolyl-2-methyl)-*N,N'*-bismethyl-1,2-ethanediamine ($L_1$, see Scheme 1) are presented. Complex **1**$(ClO_4)_4{\cdot}2H_2O$ has a $[(H_2O)Fe(\mu\text{-}O)Fe(OH_2)]^{4+}$ core unit and we show here the possibility to abstract one proton from one water molecule and to isolate the $[(H_2O)Fe(\mu\text{-}O)Fe(OH)]^{3+}$ system (**2**). This second complex is shown to be stable in solution and insensitive to further deprotonation.

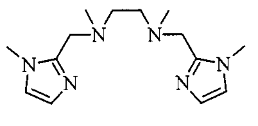

$L_1$

Scheme 1

## Results and Discussion

### X-ray Crystal Structure of $[L_1(H_2O)Fe(\mu\text{-}O)Fe(OH_2)L_1](ClO_4)_4{\cdot}2H_2O$

The structure consists of one $[L_1(H_2O)Fe(\mu\text{-}O)Fe(OH_2)L_1]^{4+}$ complex cation, four perchlorate anions and two water molecules. An ORTEP view of the cation is presented in Figure 1, and selected bond lengths and angles are listed in Table 1.

The cation possesses a crystallographicaly imposed symmetry, with the two iron atoms bridged by an oxygen atom which lies on an inversion center. The iron atom shows a pseudo-octahedral coordination with the two nonmethylated nitrogen atoms of the imidazole rings in axial positions and the two nitrogen amine atoms in equatorial positions providing the *cis*-α conformation. This conformation is also adopted by tetradentate ligands derived from the *N,N'*-bis(2-pyridylmethyl)ethane-1,2-diamine (bispicen)[14,16–20] or the very similar ligand to $L_1$ *N,N'*-bis(imidazol-4-ylmethyl)ethane-1,2-diamine in a di-Mn-di-μ-oxo complex.[21] A water molecule occupies the sixth coordination site of each iron. The two coordinated water molecules are in *trans* positions with respect to one another due to the inversion center at the bridging oxygen atom.

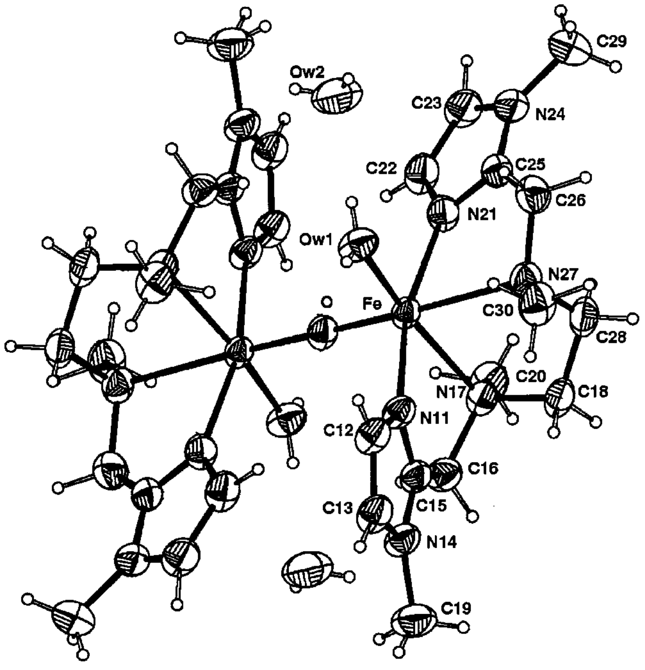

Figure 1. ORTEP view of the $[L_1(H_2O)Fe(\mu\text{-}O)Fe(OH_2)L_1]^{4+}$ cation in the crystal of compound **1**$(ClO_4)_4{\cdot}2H_2O$, showing the 50% probability thermal ellipsoids

Table 1. Selected bond lengths (Å) and angles (deg) for $[L_1(H_2O)Fe(\mu\text{-}O)Fe(OH_2)L_1]^{4+}$

| | | | |
|---|---|---|---|
| Fe−O | 1.7918(5) | Fe−N(21) | 2.084(2) |
| Fe−Ow1 | 2.052(2) | Fe−N(17) | 2.210(2) |
| Fe−N(11) | 2.125(2) | Fe−N(27) | 2.337(2) |
| O−Fe−Ow1 | 100.54(7) | N(21)−Fe−N(17) | 97.94(9) |
| O−Fe−N(21) | 97.34(7) | N(11)−Fe−N(17) | 76.77(8) |
| Ow1−Fe−N(21) | 90.3(1) | Ow1−Fe−N(27) | 86.4(1) |
| O−Fe−N(11) | 98.29(7) | N(21)−Fe−N(27) | 74.04(9) |
| Ow1−Fe−N(11) | 90.5(1) | N(11)−Fe−N(27) | 90.01(9) |
| N(21)−Fe−N(11) | 163.95(9) | N(17)−Fe−N(27) | 78.89(9) |
| O−Fe−N(17) | 96.03(7) | Fe#−O−Fe[a] | 180.0 |
| Ow1−Fe−N(17) | 160.42(9) | O−Fe−N(27) | 169.08(6) |

[a] Symmetry transformations used to generate equivalent atoms: #1−x,−y,−z+1.

The coordination at the Fe atom indicates an important deviation from octahedral geometry. The Fe atom and the four equatorial atoms form an approximate plane with a mean deviation from the respective least-squares planes of 0.2 Å. The axial nitrogen atoms N17 and N27 lie above and below the equatorial plane by 2.082(2) and −2.054(2) Å, respectively. The imidazole moieties are oriented nearly perpendicularly relative to the equatorial plane with dihedral angles 87.91(9)° and 84.7(1)°. The dihedral angle between the imidazole ring planes of 62.8(1)° indicates a significant rotation of the five-membered rings around the coordination bonds.

The two $Fe{-}N_{amine}$ distances as well as the two $Fe{-}N_{imidazole}$ distances in the $[L_1(H_2O)Fe(\mu\text{-}O)Fe(OH_2)L_1]^{4+}$ cation are not identical. Thus, Fe−N11 [2.125(2) Å] is longer than Fe−N21 [2.084(2) Å] and Fe−N27 [2.337(2) Å] is longer than Fe−N17 [2.210(2) Å]. Such an important difference between the chemically identical bonds, especially for the pair of $Fe{-}N_{amine}$ bond lengths ($\delta = 0.23$ Å) can be attributed to a *trans* effect. Indeed, the disposition of the atoms N27, the metallic centre and bridging oxygen is nearly linear with a bond angle of 169.08(6)°.

The $[(H_2O)Fe(\mu\text{-}O)Fe(OH_2)]^{4+}$ core structure has been previously obtained using the bidentate 1,10-phenanthroline (phen) ligand[22] or tetradentate ones like 2,2′:6′,2′′:6′′,2′′′-quaterpyridine (qpy),[23] tris(2-pyridylmethyl)amine (tpa),[24,25] tris[(1-methylimidazol-2-yl)methyl]amine (tmima),[26] 3-[bis(2-pyridylmethyl)amino]propionate ($bpp^-$),[27] or nitrilotriacetate ($nta^{3-}$).[28] The Fe−(μ-O) distance [1.7918(5) Å] observed here is very similar to the ones observed in the other complexes [from 1.771(5) to 1.83(1) Å]. The complex with the ligand qpy has a linear Fe−(μ-O)−Fe core structure as observed in **1**, the other cores having a bent geometry with bridging angles ranging from 153.2(6) to 177.5(5)°. The Fe···Fe separation [3.584(1) Å] in **1** is the longest among the seven complexes mentioned here.

The bond length Fe−Ow of 2.052(2) Å is in the range of those previously reported value for $Fe^{III}$ complexes coordinated by water [2.021(5)−2.19(1) Å]. The main difference lies in the torsion angle Ow−Fe···Fe−Ow which is equal, in increasing order, to 7.7° in $[(nta)(H_2O)Fe(\mu\text{-}O)Fe(H_2O)(nta)]^{2-}$, 8.8° in $[(bpp)(H_2O)Fe(\mu\text{-}O)Fe(H_2O)(bpp)]^{2+}$, 81.9° in $[(phen)_2(H_2O)Fe(\mu\text{-}O)Fe(OH_2)(phen)_2]^{4+}$, 123.0° in $[(tpa)(H_2O)Fe(\mu\text{-}O)Fe(OH_2)(tpa)]^{4+}$, 131.7° in $[(tmima)(H_2O)Fe(\mu\text{-}O)Fe(OH_2)(tmima)]^{4+}$ and 180° in **1** (not defined for $[(qpy)(H_2O)Fe(\mu\text{-}O)Fe(OH_2)(qpy)]^{4+}$ since the four atoms are aligned). The intramolecular π-π stacking of the phenanthroline rings in $[(phen)_2(H_2O)Fe(\mu\text{-}O)Fe(OH_2)(phen)_2]^{4+}$ may impose such a disposition. In the mentioned complexes, the coordinated water molecules are involved in the hydrogen bond network that may be at the origin of the variety of torsion angles observed.

As mentioned above, the studied complex crystallizes as a hydrate salt. The water molecule coordinated to the iron is involved in a strong hydrogen bond Ow1−H2w1···Ow2 with one solvent molecule [the distances Ow1···Ow2 and H2w1···Ow2 are 2.594(4) and 1.81(2) Å, respectively, and the angle at H is 174(4)°]. The other hydrogen atoms of both water molecules participate in hydrogen bonding with the perchlorate anions.

## Magnetic Susceptibility Measurements

The molar magnetic susceptibilities $\chi_M$ of a powder sample of $\mathbf{1}(ClO_4)_4 \cdot 2H_2O$ and $\mathbf{2}(ClO_4)_3 \cdot H_2O$ were measured as functions of the temperature. For **1**, $\chi_M T$ decreases from 0.74 $cm^3 \cdot mol^{-1} \cdot K$ at 300 K to a plateau at 0 below 55 K, indicating a strong antiferromagnetic coupling interaction between the two high spin $Fe^{III}$ ions ($S_1 = S_2 = 5/2$).

The same behavior was detected for **2**: at 300 K, $\chi_M T$ equals 1.40 $cm^3 \cdot mol^{-1} \cdot K$ and diminishes to reach a plateau at 0 below 35 K. The decrease of $\chi_M T$ is again characteristic of an antiferromagnetic exchange interaction between the two high spin $Fe^{III}$ sites, but the higher value of $\chi_M T$ detected at 300 K for **2** reveals a weaker coupling than in **1**.

The best fits were obtained by setting the *g* factor to 2: $J = -223$ $cm^{-1}$ for **1** and $J = -133$ $cm^{-1}$ for **2**. The *J* value calculated for **1** is of the same magnitude as the one measured for the other di-aquo-di-iron-μ-oxo complexes: −210 $cm^{-1}$ in $[(tpa)(H_2O)Fe(\mu\text{-}O)Fe(H_2O)(tpa)]^{4+}$,[24] −220 $cm^{-1}$ in $[(phen)_2(H_2O)Fe(\mu\text{-}O)Fe(OH_2)(phen)_2]^{4+}$ [22] and −228 $cm^{-1}$ in $[(bpp)(H_2O)Fe(\mu\text{-}O)Fe(OH_2)(bpp)]^{2+}$.[27]

However, the value determined for **2** is significantly less negative than the ones measured for $[(H_2O)Fe(\mu\text{-}O)Fe(OH)]^{3+}$ core complexes: −194 $cm^{-1}$ with TPA,[24] −196 $cm^{-1}$ with 5-$Et_3$-TPA[15] and −184 $cm^{-1}$ with bispic$Me_2$en.[14] This weaker coupling interaction reveals a less efficient superexchange pathway. As previously mentioned in the literature, the latter is essentially governed by the Fe−(μ-O) distances for bridging angles ranging from 120 to 180°.[29,30] It has been established that the coupling constant *J* is correlated to half of the shortest superexchange pathway between the two $Fe^{III}$ ions, designated as P according to Equation (1):

$$J = A \cdot \exp[B(P - 2)] \qquad (1)$$

with $A = -17.52$ $cm^{-1}$ and $B = -12.663$ $Å^{-1}$ if *P* is expressed in Å and *J* in $cm^{-1}$.[29,31,32] For **1**, *P* equals 1.791 Å, which gives a coupling constant of −247 $cm^{-1}$, in agreement with the value of −223 $cm^{-1}$ observed experimentally. For compound **2** it is possible to evaluate from the *J* value an average Fe−(μ-O) distance of 1.84 Å, a value slightly greater than the ones measured by X-ray diffraction studies on the three $[(H_2O)Fe(\mu\text{-}O)Fe(OH)]^{3+}$ core structures for which the *P* parameter ranges from 1.80 to 1.82 Å.[14,15,24]

One can argue that the exchange coupling constant calculated here for compound **2** is closer to the values determined for the double-bridged $[LFe(\mu\text{-}O)(\mu\text{-}OH)FeL]^{3+}$ systems {−113 $cm^{-1}$ for L = 6-$Me_3$-TPA,[19] −106 $cm^{-1}$ for L = bispic$Et_2$en,[19] −84 $cm^{-1}$ for L = bispic$Me_2$en[16] (see also remark 42 in ref. [19])}, a formulation that cannot be rejected on the basis of the elementary analysis alone. Nevertheless, as will be shown in the next section, the Raman studies support the hypothesis of a single μ-oxo bridge.

## Raman Spectra

We will focus on the frequency domain (330 to 650 $cm^{-1}$) where the symmetric stretching vibration mode of the Fe−(μ-O)−Fe core unit is expected to be detected. This vibration mode has been shown to be strongly dependent on the bridging angle,[33] and is thus indicative of the core unit geometry. In the solid state, the Raman spectrum of compound $\mathbf{1}(ClO_4)_4 \cdot 2H_2O$ exhibits a band centered at 347 $cm^{-1}$, while it is detected at 455 $cm^{-1}$ for complex $\mathbf{2}(ClO_4)_3 \cdot H_2O$. Only the acetonitrile solution of **2** was investigated and the recorded spectrum is very similar to that obtained in the solid state. The band detected at 455 $cm^{-1}$ in the solid state is shifted to 458 $cm^{-1}$ in solution. From the published correlation of the $\nu_s$ frequency as a function of the Fe−(μ-O)−Fe angle, 347 $cm^{-1}$ would correspond to a straight angle and is in good agreement with the X-ray diffraction results.

The higher frequency observed for **2** indicates a bent core structure. The double-bridged $[Fe(\mu\text{-}O)(\mu\text{-}OH)Fe]^{3+}$ cores are characterized by an even higher frequency for the symmetric vibration, around 600 $cm^{-1}$.[14,16,19] The μ-oxo-μ-hydroxo core can thus be dismissed since no signature is detected at such a high frequency. The approximate 150° bridging angle value deduced from the correlation mentioned above is slightly too high to be compatible with the presence of $H_3O_2^-$ as a second bridge, since the X-ray diffraction studies performed on such complexes lead to the determination of Fe−(μ-O)−Fe angles in the range 136−139°.[14,15,24] The likelihood of the presence of a $H_3O_2^-$ bridge is enforced, however, by the fact that the correlation we are referring to has been established for clusters presenting shorter Fe−(μ-O) distances than the one expected from the magnetic measurements. As the separation between the iron and the oxygen atoms increases, one can expect the $\nu_s$ frequency to decrease.[34] The bridging angle value of 150° may hence be an overestimation.

Both the magnetic and the Raman studies performed in the solid state support the existence in **2** of an intramolecular hydrogen bond between the coordinated water and hydroxide molecules, this interaction persisting in solution (Scheme 2).

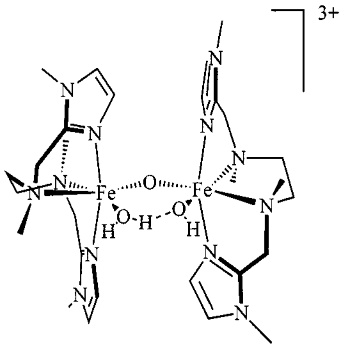

**2**

Scheme 2

### UV/Vis Absorption Spectra

The spectra of **1** [spectrum (a)] and **2** [spectrum (e)] recorded on acetonitrile solutions are shown in Figure 2.

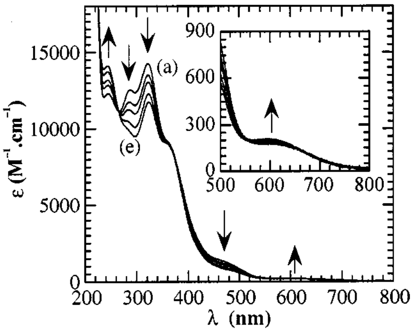

Figure 2. UV/Vis spectra of complexes $\mathbf{1}(ClO_4)_4\cdot2H_2O$ [spectrum (a)] and $\mathbf{2}(ClO_4)_3\cdot H_2O$ [spectrum (e)] dissolved in dry acetonitrile; spectra (b) to (e) correspond respectively to the addition of 0.3, 0.5, 0.8 and 1 equivalent of $Et_3N$ to a solution of **1**; the inset shows an amplification of the 500 to 800 nm region

Similar features between those two spectra may be noted. The bands at 245 nm ($\varepsilon$ = 12300 $\text{M}^{-1}\cdot\text{cm}^{-1}$ for **1** and $\varepsilon$ = 14100 $\text{M}^{-1}\cdot\text{cm}^{-1}$ for **2**) can be assigned to $\pi\rightarrow\pi^*$ transitions in the aromatic groups of the ligand. Other bands are observed at 287 nm ($\varepsilon$ = 12500 $\text{M}^{-1}\cdot\text{cm}^{-1}$ for **1**, $\varepsilon$ = 9800 $\text{M}^{-1}\cdot\text{cm}^{-1}$ sh for **2**), 323 nm ($\varepsilon$ = 14250 $\text{M}^{-1}\cdot\text{cm}^{-1}$ for **1** and $\varepsilon$ = 11750 $\text{M}^{-1}\cdot\text{cm}^{-1}$ for **2**), 365 nm ($\varepsilon$ = 8900 $\text{M}^{-1}\cdot\text{cm}^{-1}$ for **1** and **2**) and 472 nm ($\varepsilon$ = 1300 $\text{M}^{-1}\cdot\text{cm}^{-1}$ for **1** and $\varepsilon$ = 830 $\text{M}^{-1}\cdot\text{cm}^{-1}$ for **2**). The last two originate from weak oxo-to-iron LMCT transitions and, more specifically, the transition at 472 nm is assigned to the ${}^6A_1 \rightarrow ({}^4A_1, {}^4E)$ transition and is the signature of the Fe−(μ-O)−Fe motif, independent of the bridging angle value.[16,35] Another important characteristic of the μ-oxo core is expected in the 550−700 nm region, the response being strongly dependent on the Fe−(μ-O)−Fe angle: the more bent, the less energetic and/or the more intense.[36] Magnifying the 550−800 nm region reveals the existence of a low-intensity band centered around 600 nm with a molar extinction coefficient larger for **2** ($\varepsilon$ = 205 $\text{M}^{-1}\cdot\text{cm}^{-1}$) than for **1** ($\varepsilon$ = 175 $\text{M}^{-1}\cdot\text{cm}^{-1}$). A similar increase in the intensity of the absorption has been observed for the tpa complexes[16]: the band at 572 nm ($\varepsilon$ = 125 $\text{M}^{-1}\cdot\text{cm}^{-1}$) for $[\text{tpa}(H_2O)\text{Fe}(\mu\text{-O})\text{Fe}(OH_2)\text{tpa}]^{4+}$ is shifted to 608 nm ($\varepsilon$ = 165 $\text{M}^{-1}\cdot\text{cm}^{-1}$) in $[\text{tpa}(H_2O)\text{Fe}(\mu\text{-O})\text{Fe}(OH)\text{tpa}]^{3+}$. Such a behavior indicates that **2** presents a bent structure in contrast to the linear arrangement in **1**. The molar extinction coefficient value measured for **2** is in agreement with a mono-μ-oxo core unit, the protonated diamond core $[\text{Fe}(\mu\text{-O})(\mu\text{-OH})\text{Fe}]^{3+}$ being characterized by an epsilon value greater by at least a factor of three. Results from UV/Vis absorption spectroscopy thus corroborate the conclusion formulated from Raman analysis, i.e. the persistence in solution of the internal hydrogen bond in **2**.

The conversion between **1** and **2** may be achieved in solution by addition of one equivalent of triethylamine to a solution of **1**, or by addition of one equivalent of perchloric acid to a solution of **2**. Figure 2 reproduces the changes in the UV/Vis spectrum of **1** upon the addition of $Et_3N$. Three isosbestic points are detected at 260, 555 and 680 nm, supporting the existence in solution of two chromophores. Spectra (b) to (d) can indeed be reproduced by assuming a linear combination of spectra (a) and (e), the coefficient for (e) being the number *x* of equivalents of base added and the one for (a) being $(1 - x)$. This indicates that the reaction is quantitative. The same holds if $HClO_4$ is added to **2** (see Scheme 3). A parallel control of the acido-basic conversions have been performed by X-band EPR and no signal has been detected, supporting the persistence in solution of dinuclear complexes.

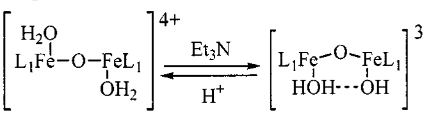

$$\left[\begin{array}{c} H_2O \\ L_1\text{Fe}{-}O{-}\text{Fe}L_1 \\ \qquad\quad OH_2 \end{array}\right]^{4+} \underset{H^+}{\overset{Et_3N}{\rightleftharpoons}} \left[\begin{array}{c} L_1\text{Fe}{-}O{-}\text{Fe}L_1 \\ HOH\cdots OH \end{array}\right]^{3+}$$

Scheme 3

It was not possible to further deprotonate compound **1** with $Et_3N$ contrary to what has been reported for the analogous phenanthroline complex.[37] This suggests that even in acetonitrile solution, the coordinated water molecule in **2** is engaged in a hydrogen bond interaction, which is in agreement with the postulated $H_3O_2^-$ bridge.

## Conclusion

We have studied here the $[L_1(H_2O)\text{Fe}(\mu\text{-O})\text{Fe}(OH_2)L_1](ClO_4)_4\cdot2H_2O$ $[\mathbf{1}(ClO_4)_4\cdot2H_2O]$ species and the associated monodeprotonated form $[L_1(H_2O)Fe(\mu\text{-}O)Fe(OH)L_1](ClO_4)_3{\cdot}H_2O$ [**2**$(ClO_4)_3{\cdot}H_2O$]. The two complexes have been characterized by different spectroscopic techniques such as UV/Vis and Raman. Compound **1**$(ClO_4)_4{\cdot}2H_2O$ has, moreover, been characterized by an X-ray diffraction study. The interconversion between **1** and **2** by addition of one equivalent of base or acid has been followed by UV/Vis absorption spectroscopy. No evolution towards a di-bridged system in a dry acetonitrile solution has been noted for **2** contrary to what has been observed for other $[(H_2O)Fe(\mu\text{-}O)Fe(OH)]^{3+}$ systems containing coordinated pyridine groups.[14,15] The generation of the diamond core structure seems to be related to the lability of the coordinated water molecule and the nature of the polydentate ligand. Imidazole is a stronger σ-donor and weaker π-acceptor ligand than pyridine. This could be the origin of the elongation of the Fe−(μ-O) bond that is suggested from magnetic susceptibility and Raman data. The $Fe^{III}$ ions could thus be less electrophilic when coordinated to imidazoles instead of pyridines, and less sensitive to a nucleophilic attack of the coordinated hydroxide ion, preventing the formation of the protonated diamond core structure.

## Experimental Section

**General Remarks:** Reagents and solvents were purchased commercially and used as received. Acetonitrile used for solution studies was distilled before use and dried on an alumina column. The synthesis of *N,N′*-dimethyl-*N,N′*-bis(1-methylimidazol-2-ylmethyl)-ethane-1,2-diamine ($L_1$) has been described previously.[38]

***Caution!*** *Perchlorate salts of metal complexes with organic ligands are potentially explosive. Only small quantities of these compounds should be prepared and handle behind suitable protective shields.*

**$[L_1(H_2O)Fe(\mu\text{-}O)Fe(OH_2)L_1](ClO_4)_4{\cdot}X$ [X = $2H_2O$, 1$(ClO_4)_4{\cdot}2H_2O$; X = $C_2H_5OH$, 3$(ClO_4)_4{\cdot}C_2H_5OH{\cdot}H_2O$]:** An ethanol/water solution (1:1, 5 mL) containing $L_1$ (138 mg, 0.5 mmol) was mixed with one equivalent of sodium hydroxide (0.1 mL of a 5 M solution). $Fe(ClO_4)_3{\cdot}6H_2O$ (232 mg, 0.5 mmol) dissolved in 2 mL of water was then added. An orange precipitate appeared that was then filtered and washed with water to give138 mg of product (48% yield versus Fe). When $Fe(ClO_4)_3{\cdot}6H_2O$ was added as an ethanolic solution, an orange precipitate was also formed. In both cases orange crystals were obtained by slow evaporation of an acetonitrile solution differing only in the nature of the solvation molecules. − $[L_1(H_2O)Fe(\mu\text{-}O)Fe(OH_2)L_1](ClO_4)_4{\cdot}C_2H_5OH{\cdot}H_2O$ ($C_{30}H_{60}Cl_4Fe_2N_{12}O_{21}$, 1178.38): calcd. C 30.58, H 5.13, N 14.26, Cl 12.03; found C 30.47, H 5.05, N 14.06, Cl 12.00.

**$[L_1(H_2O)Fe(\mu\text{-}O)Fe(OH)L_1](ClO_4)_3{\cdot}H_2O$ (2$(ClO_4)_3{\cdot}H_2O$):** To 10 mL of a methanolic degassed solution containing $L_1$ (138 mg, 0.5 mmol) and triethylamine (0.139 mL, 1.0 mmol) was added, under an argon atmosphere, 5 mL of a degassed methanolic solution of $Fe(ClO_4)_3{\cdot}6H_2O$ (232 mg, 0.5 mmol). A small argon gas current was maintained overnight and tiny brownish green crystals were obtained (95 mg, 37% yield versus Fe). They were too small to allow an X-ray diffraction measurement. − $[L_1(H_2O)Fe(\mu\text{-}O)Fe(OH)L_1](ClO_4)_3{\cdot}H_2O$ ($C_{28}H_{53}Cl_3Fe_2N_{12}O_{16}$, 1031.85): calcd. C 32.59, H 5.17, N 16.29; Cl, 10.31; found C 32.64, H 5.11, N 16.01; Cl, 10.62.

**Raman Spectroscopy:** Raman spectra were recorded on a Jobin-Yvon double monochromator $U_{1000}$ equipped with an As/Ga photomultiplier and photocounting detection. The excitation wavelength line was the 413.1 nm line of a $Kr^+$ laser at 10−15 mW incident power level. Solid samples of compounds **1**$(ClO_4)_4{\cdot}2H_2O$ and **2**$(ClO_4)_3{\cdot}H_2O$ were mounted on a disk rotating at about 1000 rpm. The spectral width was 4 $cm^{-1}$. The solution sample of **2** was transferred in a degassed rotating cell. The spectral resolution was 6 $cm^{-1}$.

**Magnetic Susceptibility Measurements:** Magnetic susceptibility data were recorded on a MPMS5 magnetometer (Quantum Design Inc.). The calibration was made at 298 K using a palladium reference sample furnished by Quantum Design Inc. The data were collected over a temperature range of 10−300 K at a magnetic field of 1.0 T and were corrected for diamagnetism. The $\chi_M T$ vs. $T$ curves were fitted using the van Vleck formula where the same $g$ factor was assumed for each spin state $S$. The energies appearing in the exponential arguments are derived from the Heisenberg-van Vleck-Dirac Hamiltonian $-J\boldsymbol{S_1}{\cdot}\boldsymbol{S_2}$. The total spin $S$ runs from $|S_1 - S_2|$ to $S_1 + S_2$ by unit steps.

**EPR Spectroscopy:** EPR spectra were recorded on Bruker ER 200 D and 300 spectrometers at X-band. For low temperature studies, an Oxford Instrument continuous-flow liquid helium cryostat and a temperature control system were used.

**UV/Vis Spectroscopy:** UV/Vis spectra were recorded on a Varian Cary 5E spectrophotometer.

**X-ray Crystallographic Study:** **1**$(ClO_4)_4{\cdot}2H_2O$ ($C_{28}H_{56}Cl_4Fe_2N_{12}O_{21}$; $M$ = 1150.33 $g{\cdot}mol^{-1}$) crystallizes in the orthorhombic space group $P_{bca}$ with $a$ = 17.101(2) Å, $b$ = 13.824(3) Å, $c$ = 20.922(6) Å and $\alpha = \beta = \gamma = 90°$, $Z$ = 8, $d$ = 1.545 $g{\cdot}cm^{-3}$. The unit-cell and intensity data were measured with an Enraf−Nonius CAD-4 diffractometer with graphite monochromated Mo-$K_\alpha$ radiation ($\lambda$ = 0.71073 Å). A prismatic orange crystal of $[L_1(H_2O)Fe(\mu\text{-}O)Fe(OH_2)L_1](ClO_4)_4{\cdot}2H_2O$ with the dimensions 0.53 × 0.33 × 0.25 mm was chosen for the X-ray diffraction measurement. The cell constants were obtained by least-squares procedures based upon the 2Θ values of 25 reflections measured in the range $22.0 < 2\Theta < 23.7°$ at ambient temperature. During data collection, three control reflections were measured every three hours. The crystal was stable and the check reflections showed a negligible decay in intensity of 0.45% during all the X-ray data collection. A total of 8682 reflections were collected in the range $4.26 < 2\Theta < 50.0°$ within [$-20 \le h \le 20$, $0 \le k \le 16$, $0 \le l \le 24$]. From 4348 independent reflections, 2867 were considered as observed [$I > 2\sigma(I)$]. The structure was solved by direct methods with the program SHELXS-86[39] and refined by using the SHELXL-93[40] program. The molecular cation was located in a special crystallographic position with the oxygen atom at an inversion center (0,0,0.5). The perchlorate anions were located in a general crystallographic position. The observed disorder in the structure involved the anions; both perchlorates were disordered over two sites with nonidentical occupations (0.74 and 0.26; 0.70 and 0.30). The structure was refined anisotropically (non-hydrogen atoms) by full-matrix least-squares approximation based on $F^2$. The hydrogen atoms at the oxygen atoms of water molecules were localized in a difference Fourier synthesis and refined isotropically. Other hydrogen atom positions were calculated by assuming geometrical positions and were included in the structural model. The final weighting scheme was $w = 1/[\sigma^2(F_o^2) + (0.0568\,P)^2 + 0.001\,P]$, where $P = (F_o^2 + 2F_c^2)/3$. The final refinement of this model was continued until convergence when $R1 = 0.0360$ for $F^2 > 2\sigma(F^2)$ and $R_w$ =

0.0840 were reached. The final difference map showed the largest residual peaks of 0.398 and $-0.169$ e·Å$^{-3}$. The two largest peaks were found at the Fe atoms.

Crystallographic data (excluding structure factors) for the structure(s) included in this paper have been deposited with the Cambridge Crystallographic Data Centre as supplementary publication no. CCDC-143394. Copies of the data can be obtained free of charge on application to CCDC, 12 Union Road, Cambridge CB2 1EZ, UK [Fax: (internat.) + 44-1223/336-033; E-mail: deposit@ccdc.cam.ac.uk].

## Acknowledgments

We are grateful to Prof. Jean-Baptiste Verlhac for providing us with the precursors of the ligand $L_1$.

---

[1] B. J. Wallar, J. D. Lipscomb, *Chem. Rev.* **1996**, *96*, 2625−2657.
[2] E. I. Solomon, T. C. Brunold, M. I. David, J. N. Kemsley, S.-K. Lee, N. Lehnert, F. Neese, A. J. Skulan, Y.-S. Yang, J. Zhou, *Chem. Rev.* **2000**, *100*, 235−349.
[3] A. C. Rosenzweig, C. A. Frederick, S. J. Lippard, P. Nordlund, *Nature* **1993**, *366*, 537−543.
[4] A. C. Rosenzweig, P. Nordlund, P. M. Takahara, C. A. Frederick, S. J. Lippard, *Chem. Biol.* **1995**, *2*, 409−418.
[5] N. Elango, R. Radhakrishnan, W. A. Froland, B. J. Wallar, C. A. Earhart, J. D. Lipscomb, D. H. Ohlendorf, *Protein Sci.* **1997**, *6*, 556−568.
[6] S. K. Lee, J. D. Lipscomb, *Biochemistry* **1999**, *38*, 4423−4432.
[7] T. C. Brunold, N. Tamura, N. Kitajima, Y. Moro-oka, E. I. Solomon, *J. Am. Chem. Soc.* **1998**, *120*, 5674−5690.
[8] S. K. Lee, J. C. Nesheim, J. D. Lipscomb, *J. Biol. Chem.* **1993**, *268*, 21569−21577.
[9] Y. Liu, J. C. Nesheim, S. K. Lee, J. D. Lipscomb, *J. Biol. Chem.* **1995**, *270*, 24662−24665.
[10] K. E. Liu, A. M. Valentine, D. Qiu, D. E. Edmonson, E. H. Appelman, T. G. Spiro, S. J. Lippard, *J. Am. Chem. Soc.* **1995**, *117*, 4997−4998.
[11] K. E. Liu, D. Wang, B. H. Huynh, D. E. Edmonson, A. Salifoglou, S. J. Lippard, *J. Am. Chem. Soc.* **1994**, *116*, 7465−7466.
[12] L. Shu, J. C. Nesheim, K. Kauffmann, E. Münck, J. D. Lipscomb, L. Que, Jr., *Science* **1997**, *275*, 515−518.
[13] J. C. Nesheim, J. D. Lipscomb, *Biochemistry* **1996**, *35*, 10240−10247.
[14] S. Poussereau, G. Blondin, M. Cesario, J. Guilhem, G. Chottard, F. Gonnet, J.-J. Girerd, *Inorg. Chem.* **1998**, *37*, 3128−3132.
[15] Y. Dong, H. Fujii, M. P. Hendrich, R. A. Leising, G. Pan, C. R. Randall, E. C. Wilkinson, Y. Zang, L. Que, Jr., B. G. Fox, K. Kauffmann, E. Münck, *J. Am. Chem. Soc.* **1995**, *117*, 2778−2792.
[16] R. Hazell, K. B. Jensen, C. J. McKenzie, H. Toftlund, *J. Chem. Soc., Dalton Trans.* **1995**, 707−717.
[17] N. Arsulamy, P. A. Goodson, D. J. Hodgson, J. Glerup, K. Michelsen, *Inorg. Chim. Acta* **1994**, *216*, 21−29.
[18] T. Okuno, S. Ito, S. Ohba, Y. Nishida, *J. Chem. Soc., Dalton Trans.* **1997**, 3547−3551.
[19] H. Zheng, Y. Zang, Y. Dong, V. G. Young, Jr., L. Que, Jr., *J. Am. Chem. Soc.* **1999**, *121*, 2226−2235.
[20] J. Simaan, S. Poussereau, G. Blondin, J.-J. Girerd, D. Defaye, C. Philouze, J. Guilhem, L. Tchertanov, *Inorg. Chim. Acta* **2000**, *299*, 221−230.
[21] Y.-M. Frapart, A. Boussac, R. Albach, E. Anxolabéhère-Mallart, M. Delroisse, J.-B. Verlhac, G. Blondin, J.-J. Girerd, J. Guilhem, M. Césario, A. W. Rutherford, D. Lexa, *J. Am. Chem. Soc.* **1996**, *118*, 2669−2678.
[22] J. E. Plowman, T. M. Loehr, C. K. Schauer, O. P. Anderson, *Inorg. Chem.* **1984**, *23*, 3553−3559.
[23] F. Calderazzo, L. Labella, F. Marchetti, *J. Chem. Soc., Dalton Trans.* **1998**, 1485−1489.
[24] A. Hazell, K. B. Jensen, C. J. McKenzie, H. Toftlund, *Inorg. Chem.* **1994**, *33*, 3127−3134.
[25] B. R. Whittlesey, Z. Pang, R. A. Holwerda, *Inorg. Chim. Acta* **1999**, 124−126.
[26] R. M. Buchanan, S. Chen, J. F. Richardson, M. Bressan, L. Forti, A. Morvillo, R. H. Fish, *Inorg. Chem.* **1994**, *33*, 3208−3209.
[27] A. Hazell, K. B. Jensen, C. J. McKenzie, H. Toftlund, *J. Chem. Soc., Dalton Trans.* **1993**, 3249−3257.
[28] S. L. Heath, A. K. Powell, H. L. Utting, M. Helliwell, *J. Chem. Soc., Dalton Trans.* **1992**, 305−307.
[29] S. M. Gorun, S. J. Lippard, *Inorg. Chem.* **1991**, *30*, 1625−1630.
[30] R. Hotzelmann, K. Wieghardt, U. Flörke, H.-J. Haupt, D. C. Weatherburn, J. Bonvoisin, G. Blondin, J.-J. Girerd, *J. Am. Chem. Soc.* **1992**, *114*, 1681−1696.
[31] The equation given in ref 19 in erroneous in the exponential argument.
[32] H. Weihe, H. U. Güdel, *J. Am. Chem. Soc.* **1997**, *119*, 6539−6543.
[33] J. Sanders-Loehr, W. D. Wheeler, A. K. Shiemke, B. A. Averill, T. M. Loehr, *J. Am. Chem. Soc.* **1989**, *111*, 8084−8093.
[34] R. M. Wing, K. P. Callahan, *Inorg. Chem.* **1969**, *8*, 871−874.
[35] R. C. Reem, J. M. McCormick, D. E. Richardson, F. J. Devlin, P. J. Stephens, R. L. Musselman, E. I. Solomon, *J. Am. Chem. Soc.* **1989**, *111*, 4688−4704.
[36] R. E. Norman, R. C. Holz, S. Ménage, C. J. O'Connor, J. H. Zhang, L. Que, Jr., *Inorg. Chem.* **1990**, *29*, 4629−4637.
[37] C. Duboc-Toia, S. Ménage, J.-M. Vincent, M. T. Averbuch-Pouchot, M. Fontecave, *Inorg. Chem.* **1997**, *36*, 6148−6149.
[38] D. Tétard, J.-B. Verlhac, *Journal of Molecular Catalysis A: Chemical* **1996**, *113*, 223−230.
[39] G. M. Sheldrick, *Acta Crystallogr., Sect. A* **1990**, *46*, 467.
[40] G. M. Sheldrick, Program for the refinement of crystal structures, University of Göttingen, Germany.

Received September 8, 2000
[I00338]